



OPEN CT-Derived spleen volume accurately diagnoses severe portal hypertension at HVPg thresholds of 16 mmHg

Xinyu Chen^{1,5}, Jiamei Zhou^{2,3,5}, Yicheng Lin^{1,5}, Kefeng Jia^{4,5}, Jiajun Tian^{4,5}, Fenghui Li^{4,5}, Rong Lv⁴, Weili Yin⁴, Fang Wang⁴, Ping Zhu⁴, Chao Yang⁴, Jiayin Wang⁴, Tao Wang⁴, Junqing Yan⁴, Ying Liu⁴, Qing Ye^{3,4}✉ & Huiling Xiang^{3,4}✉

To investigate the diagnostic utility of a noninvasive method based on spleen volume for the accurate diagnosis of severe portal hypertension (PH). We enrolled 260 patients undergoing hepatic venous pressure gradient (HVPg) assessment and enhanced CT at Tianjin Third Central Hospital (December 2019–July 2023), with clinical data collected. Patients were stratified by HVPg levels: ≥ 16 mmHg (severe PH group) and < 16 mmHg (non-severe PH group). We included 120 cirrhotic patients who met the inclusion criteria. Splenic volume exhibited a linear correlation with HVPg ($r = 0.364$, $p < 0.001$). Univariate and multivariate logistic regression analyses identified spleen volume, age, and serum albumin as independent risk factors for severe PH ($p < 0.05$). Accordingly, a clinical diagnostic model was developed, named the “S-HVPg” score. The area under the curve (AUC) for the “S-HVPg” score was 0.803, with an optimal threshold of 0.694, achieving sensitivity, specificity, positive predictive value (PPV), and negative predictive value (NPV) of 78.8%, 74.3%, 88.2%, and 59.1%, respectively. The spleen volume-based “S-HVPg” scoring system introduces a novel, straightforward, noninvasive approach for diagnosing severe PH. A cutoff value of 0.694 for the S-HVPg score effectively distinguishes patients with severe PH from those with cirrhosis.

Keywords Cirrhosis, Portal hypertension, Spleen volume, Hepatic venous pressure gradient, Diagnostic model

Cirrhosis develops following prolonged inflammation, where healthy liver tissue is progressively replaced by fibrous tissue and regenerative nodules, leading to portal hypertension¹. Portal hypertension resulting from cirrhosis can lead to severe complications such as variceal hemorrhage, ascites, and hepatic encephalopathy^{2–4}. Hepatic venous pressure gradient (HVPg) serves as the gold standard for assessing portal pressure^{5,6}. Cirrhotic patients with HVPg ≥ 16 mmHg were considered to be severe PH. HVPg ≥ 16 mmHg indicates portal hypertension with an increased risk of mortality, predisposing patients to complications associated with difficult-to-control or recurrent decompensated cirrhosis. It is a robust predictor of poor prognosis and signifies a significantly heightened mortality risk among patients with cirrhotic portal hypertension^{7,8}. HVPg ≥ 16 mmHg has also been linked to increased short-term mortality in patients undergoing non-hepatic abdominal surgeries⁵. However, HVPg measurement has inherent drawbacks: (1) it requires skilled operators and specialized hospital facilities; (2) it is costly and invasive; (3) it poses challenges in monitoring patient dynamics^{9–11}. Consequently, there is a growing interest in developing simpler, non-invasive approaches for diagnosing and monitoring portal hypertension in patients with hepatic disorders¹². Several noninvasive imaging-based tests have been proposed, including computed tomography (CT)-based assessments of liver and spleen volumes to predict HVPg in

¹The Third Central Clinical College of Tianjin Medical University, Tianjin University Central Hospital (Tianjin Third Central Hospital), Tianjin Key Laboratory of Extracorporeal Life Support for Critical Diseases, Institute of Hepatobiliary Disease, Tianjin, China. ²Tianjin Union Medical Center, Tianjin Medical University, Tianjin, China. ³Department of Gastroenterology, The Second Central Hospital of Baoding, Zhuozhou, Hebei, China. ⁴Tianjin University Central Hospital(Tianjin Third Central Hospital), Department of Gastroenterology and Hepatology, Tianjin Key Laboratory of Extracorporeal Life Support for Critical Diseases, Institute of Hepatobiliary Disease, No 83, Jintang road, Hedong district, Tianjin, China. ⁵AQXinyu Chen, Jiamei Zhou, Yicheng Lin, Kefeng Jia, Jiajun Tian and Fenghui Li contributed equally. ✉email: yeqing022@163.com; huilingxiang@163.com

patients with hepatocellular carcinoma and cirrhosis, enabling accurate diagnosis of clinically significant portal hypertension^{9,13,14}. However, previous studies have predominantly focused on clinically significant portal hypertension in patients with cirrhosis or hepatocellular carcinoma, using HVP ≥ 10 mmHg as the diagnostic threshold, with fewer studies addressing the noninvasive diagnosis of portal hypertension across varying severities in cirrhotic patients¹⁵.

This study aims to explore the correlation between spleen volume and HVP in cirrhotic patients, develop a noninvasive model for diagnosing severe PH, and assess the accuracy of this model.

Patients and methods

Study population

Study Population: This retrospective study included patients who visited the Third Central Hospital of Tianjin, China, between December 2019 and July 2023 for HVP testing ($N = 203$).

Inclusion Criteria: (1) age above or equal to 18-year-old; (2) undergoing HVP measurements and enhanced CT examination; (3) Patients diagnosed with cirrhosis (according to the diagnostic criteria of the Guidelines for the Diagnosis and Treatment of Cirrhosis of the Liver, 2020 edition)¹⁶; (4) Availability of complete clinical data.

Exclusion Criteria: (1) Patients who underwent HVP measurements and CT examination more than 3 months apart; (2) previous treatment with splenectomy, liver surgery, transjugular intrahepatic portosystemic shunt, or liver transplantation; (3) diagnosis of hepatocellular carcinoma; (4) non-sinusoidal portal hypertension (e.g., idiopathic portal hypertension, Budd-Chiari syndrome)⁴;

Grouping Methods: Patients were classified based on HVP ≥ 16 mmHg^{5,7}, dividing them into a group with severe portal hypertension (PH) and a group with non-severe PH¹⁷.

Study method

HVP measurements

HVP measurements were performed by an experienced interventional radiologist using the Seldinger technique via the right internal jugular vein. A catheter sheath and 5.5 F Fogarty balloon catheter were advanced to the main trunk of the right hepatic vein branch (approximately 4 cm from the opening), with three measurements taken and the average recorded as the representative HVP. HVP was calculated as the difference between the wedged hepatic venous pressure (WHVP) and the free hepatic venous pressure (FHVP). The HVP formula used was $HVP = WHVP - FHVP$ ¹⁸.

Abdominal enhanced CT examination and spleen volume measurement

All patients underwent imaging using the Siemens Healthcare Definition Flash dual-source CT scanner, covering the area from the top of the diaphragm to the lower edge of the liver and spleen. The scanning parameters included a layer thickness of 5.0 mm, layer spacing of 5.0 mm, pitch of 1.375:1, voltage of 120 kVp, and current of 250 mAs. A total of 90 ml of iodine contrast agent was administered via the antecubital vein at a rate of 2.5–3.0 ml/s. Dynamic scanning was conducted in three phases: arterial (25–30 s), portal venous (70–75 s), and delayed (3 min). Subsequently, thin-layer reconstruction was performed with a reconstructed layer thickness and spacing of 1.25 mm, along with parallel coronal and sagittal image reconstructions.

The spleen was outlined in 5-mm-thick portal venous phase images acquired through continuous spiral scanning, using 3D Slicer software by two medical students (Fig. 1). A radiologist provided guidance to the students, supervised their work, and verified the measurements.

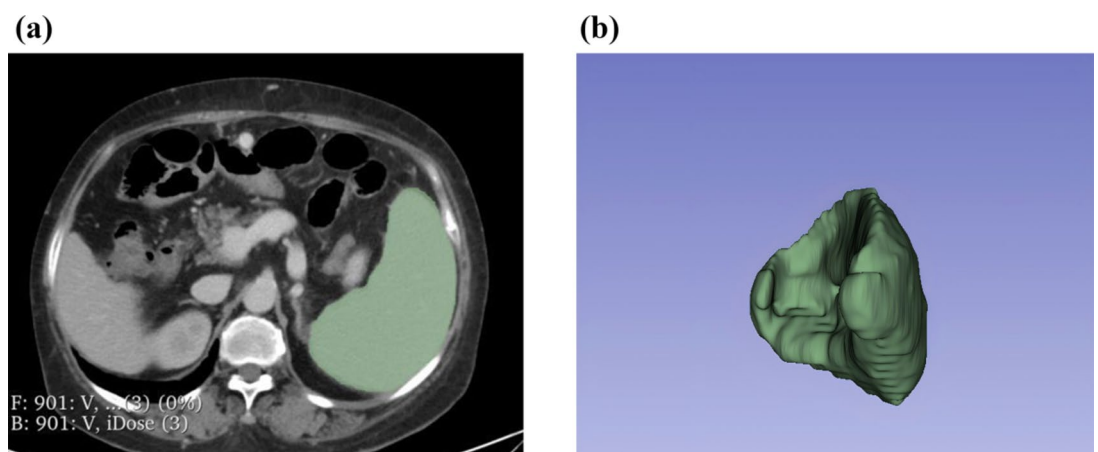


Fig. 1. Spleen volume segmentation using 3D Slicer software. **(a)** Axial image displaying spleen organ segmentation (green), overlaid on a CT scan image. **(b)** Three-dimensional segmentation of the spleen. CT: computed tomography.

Laboratory-Clinical-Endoscopic profiling evaluations

General patient data, including age, gender, height, hospitalization diagnosis, and treatment history, were recorded for all included patients. Clinical indices collected included platelets (PLT), hemoglobin (HB), International Normalized Ratio (INR), aspartate transaminase (AST), alanine transaminase (ALT), albumin (ALB), total bilirubin (TBIL), urea, and creatinine. Additionally, liver function scores such as the Child-Pugh score, Albumin-Liverin (ALBI) score, and AAR score were calculated based on clinical data.

The grading criteria for esophagogastric varices follow the criteria established by the Japan Society for Portal Hypertension¹⁹. Endoscopic indicators associated with high bleeding risk in varices were characterized by the presence of prominent bluish vascular protrusions (classified as F2 or F3) exhibiting substantial red color signs on their luminal surfaces²⁰. The patients were stratified into high-risk and low-risk groups for esophagogastric variceal hemorrhage based on the criteria above.

Calculation method of relevant scores and parameters

$ALBI = 0.66 \times \log_{10} \text{bilirubin } (\mu\text{mol/L}) - 0.085 \times \text{albumin } (\text{g/L})$; $AAR = AST/ALT$.

Statistical analysis

Data were analyzed using R 4.3.1, SPSS 27.0, and GraphPad Prism 10. Descriptive statistics were used to summarize the data. Normally distributed data are presented as mean \pm standard deviation ($\bar{x} \pm s$) and were compared using the paired t-test. Non-normally distributed data are presented as median (interquartile range, IQR) and were compared using the Mann-Whitney U test. Categorical data were compared using the χ^2 test. Spearman's correlation coefficient assessed the relationships between variables. Influence factor analysis was conducted using logistic regression models to determine odds ratios (ORs) and 95% confidence intervals (CIs) for risk factors. Sensitivity, specificity, PPV, and NPV were calculated to evaluate parameter diagnostic efficacy. Receiver operating characteristic (ROC) curves assessed model discriminatory power, calculating area under the curve (AUC) values. Calibration curves evaluated model calibration, and the Hosmer-Lemeshow goodness-of-fit test assessed model precision. Decision curves compared net clinical benefits among models. Internal validation used bootstrapping for model accuracy assessment. Statistical significance was set at $P < 0.05$.

Model validation

To assess the accuracy of the diagnostic model, internal validation was performed using bootstrap sampling²¹. The process of internal validation included the following steps: (a) Resampling: A resampled dataset of the same size as the original model development cohort was generated using bootstrap sampling as the training set. (b) Model Training: The diagnostic model was fully trained using the resampled training set, and its performance was evaluated within this training set. (c) Performance Assessment: The performance of the trained model was then assessed using the original model development cohort, and the difference in performance between the two models was computed as the bias estimate. (d) Iteration: This process was repeated 100 times to generate 100 bias estimates. The average of these bias estimates provided an adjusted bias estimate. (e) Performance Calculation: The adjusted bias estimate was subtracted from the fitted value of the performance in the original data, yielding the model's performance in internal validation²². Compared to traditional randomization validation methods, bootstrap resampling validation optimizes data utilization efficiency and mitigates issues associated with small validation sample sizes²².

Results

Study process

A total of 260 patients underwent HVPG measurements from December 2019 to July 2023. Exclusions included 7 patients without cirrhosis, 82 with portal vein thrombosis, 25 with non-sinusoidal portal hypertension, 10 with hepatocellular carcinoma, 6 who had undergone splenectomy, and 10 with poor quality abdominal CT scans. Ultimately, 120 cases were included in the study. The patient selection process is illustrated in Fig. 2.

Patient characteristics

The median age of all patients was 57.50 years (IQR 48.33–64.00). There were 78 male patients (65.00%) and 42 female patients (35.00%). The etiology included viral cirrhosis in 48 patients (40.00%), alcoholic cirrhosis in 33 patients (27.50%), and other etiologies such as non-alcoholic fatty cirrhosis and cryptogenic cirrhosis in 39 patients (32.5%). The median HVPG was 19.0 mmHg (IQR 15.0–22.0) in the total cohort. All patients had a median MELD score of 12.0 (IQR 6.0–12.0). Child-Pugh grading showed class A in 48 patients (40.00%), class B in 57 patients (47.50%), and class C in 15 patients (12.50%). Median spleen volume was 719.24 cm³ (IQR 504.35–952.98) (Table 1).

Using HVPG ≥ 16 mmHg as the criterion, patients were categorized into two groups: severe PH ($n = 85$) and non-severe PH ($n = 35$). Both groups were compared for etiology, HB, INR, ALB, HVPG, MELD score, splenic volume, bleeding risk of esophageal varices, and bleeding risk of gastric varices all showing statistically significant differences (P values < 0.05).

Relationship analysis between spleen volume and HVPG

Spleen volume showed a moderate positive correlation with HVPG ($r = 0.364$, $p < 0.001$) (Fig. 3).

Univariate and multivariate logistic regression analysis of Observational Indicators and severe PH

A univariate logistic regression analysis was conducted with severe PH as the dependent variable and clinical and imaging indicators of cirrhotic patients as independent variables to assess their correlations (Table 2). The

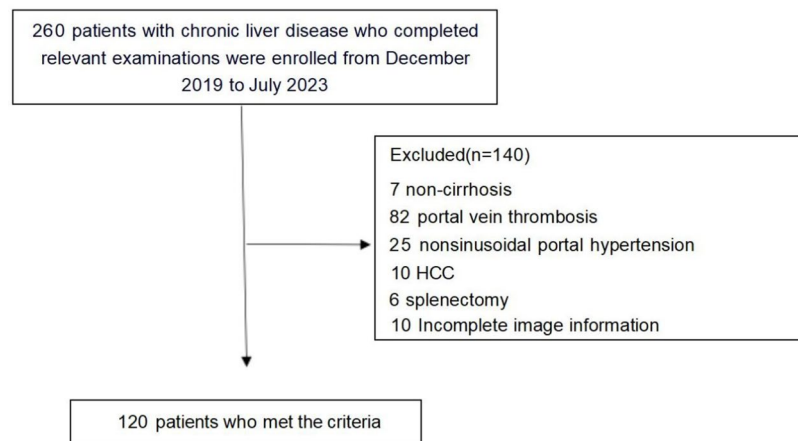


Fig. 2. Patient selection procedure. HCC, hepatocellular carcinoma.

Variable	Total (n = 120)	Non-severe PH (n = 35)	Severe PH (n = 85)	P-value
Age, years	57.5 (48.3–64.0)	57.0 (44.0–62.0)	57.3 ± 10.3	0.139
Male	78 (65.0)	21 (60.0)	57 (67.1)	0.461
Etiology				0.020
Viral hepatitis	48 (40.0)	16 (45.7)	32 (37.7)	
HBV	40 (33.3)	14 (40.0)	26 (30.6)	
HCV	8 (6.7)	2 (5.7)	6 (7.1)	
Alcohol-related	33 (27.5)	3 (8.6)	30 (35.3)	
Other	39 (32.5)	15 (42.9)	23 (27.1)	
Laboratory parameters				
Platelets, ×10 ⁹ /L	73.5 (50.0–98.8)	85.0 (52.0–125.0)	68.0 (49.5–91.0)	0.065
Hemoglobin, g/L	102.0 ± 29.4	124.0 (85.0–133.0)	97.5 ± 27.5	0.007
INR	1.3 (1.1–1.4)	1.2 (1.1–1.3)	1.3 (1.2–1.4)	0.008
Albumin, g/L	35.5 ± 6.1	38.7 ± 6.0	34.1 ± 5.6	< 0.001
ALT, U/L	20.0 (14.0–28.0)	22.0 (16.0–38.0)	20.0 (13.0–26.0)	0.227
AST, U/L	30.0 (23.0–41.0)	28.0 (21.0–39.0)	32.0 (23.0–41.0)	0.274
Bilirubin, μmol/L	23.7 (17.2–40.6)	21.2 (15.8–35.2)	25.2 (17.3–42.2)	0.299
Urea, mmol/L	4.9 (3.8–6.9)	4.8 (3.9–5.5)	5.1 (3.8–7.1)	0.448
Creatinine, μmol/L	63.0 (55.0–77.8)	63.0 (55.0–76.0)	63.0 (53.5–80.5)	0.968
HVPG, mmHg	19.0 (15.0–22.0)	10.0 (8.0–14.0)	21.0 (18.5–23.0)	< 0.001
MELD score	12.0 (6.0–12.0)	12.0 (12.0–12.0)	12.0 (6.0–12.0)	0.045
Child-Pugh grade				0.068
A (scores 5–6)	48 (40.0)	19 (54.3)	29 (34.1)	
B (scores 7–9)	57 (47.5)	15 (42.8)	42 (49.4)	
C (scores 10–15)	15 (12.5)	1 (2.9)	14 (16.5)	
Spleen volume, cm ³	719.24 (504.35–952.98)	615.85 ± 308.59	779.76 (567.96–1041.13)	0.005
Endoscopic parameters				
bleeding risk of esophageal varices				0.003
low risk	32 (28.57)	16 (48.48)	16 (20.25)	
high risk	80 (71.43)	17 (51.52)	63 (79.75)	
bleeding risk of gastric varices				0.005
low risk	39 (34.82)	18 (54.55)	21 (26.58)	
high risk	73 (65.18)	15 (45.45)	58 (73.42)	

Table 1. Baseline characteristics of the study population. Data are expressed as n/N (%), mean (SD) or median [IQR]. Abbreviations: ALT, alanine aminotransferase; AST, aspartate aminotransferase; INR, international normalized ratio; HVPG, hepatic venous pressure gradient; MELD, Model of End-stage Liver Disease.

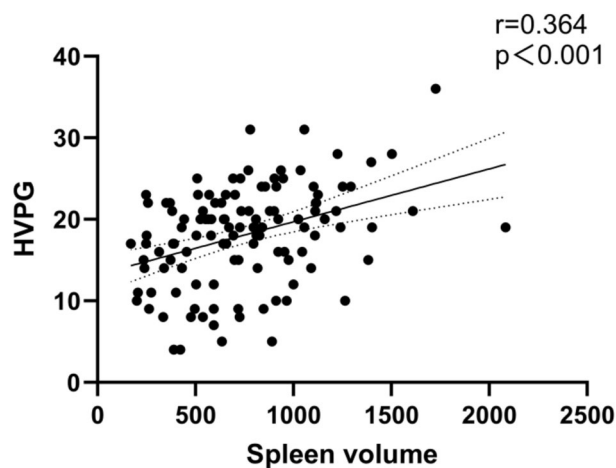


Fig. 3. Spleen volume exhibited a linear correlation with HVPG in the experimental group.

	Univariate		Multivariate	
Variable	OR (95% CI)	P Value	OR (95% CI)	p Value
Age	1.038(1.002,1.076)	0.040	1.054 (1.004,1.106)	0.033
Sex (M vs. F)	1.357 (0.602,3.602)	0.462		
Platelets	0.989(0.980,0.999)	0.025	0.996 (0.984,1.008)	0.528
Hemoglobin	0.981 (0.967,0.995)	0.010	0.998 (0.978,1.017)	0.811
INR	9.589 (1.268, 72.483)	0.028	2.700 (0.249,29.242)	0.414
Albumin	0.875 (0.813,0.942)	< 0.001	0.877 (0.782,0.984)	0.026
ALT	0.995(0.988,1.002)	0.149		
AST	0.995(0.989,1.001)	0.105		
Bilirubin	0.997 (0.991,1.004)	0.423		
Urea	1.064(0.918,1.232)	0.409		
Creatinine	1.004(0.987,1.021)	0.649		
Spleen volume	1.002(1.000,1.003)	0.008	1.002(1.001,1.004)	0.041
bleeding risk of esophageal varices				
low risk	1.00 (Reference)	—	1.00 (Reference)	—
high risk	3.706 (1.544 ~ 8.898)	0.003	2.251 (0.695,7.287)	0.176
bleeding risk of gastric varices				
low risk	1.00 (Reference)	—	1.00 (Reference)	—
high risk	3.314 (1.420 ~ 7.737)	0.006	2.312 (0.750,7.127)	0.144

Table 2. Univariate and multivariate analysis of factors associated with severe PH. Abbreviations: ALT, alanine aminotransferase; AST, aspartate aminotransferase; PT, prothrombin time; INR, international normalized ratio.

	Optimal threshold	AUC (95% CI)	Sensitivity (%)	Specificity (%)	PPV	NPV
S-HVPG score	0.694	0.803 (0.708–0.899)	78.8	74.3	88.2%	59.1%
Spleen volume	638.48	0.663 (0.555–0.772)	69.4	60.0	80.8%	44.7%
CP grade	1.50	0.629 (0.524–0.735)	65.9	54.3	77.8%	39.6%
MELD	9.00	0.606 (0.501–0.711)	91.4	34.1	36.4%	90.6%
ALBI	−1.842	0.706 (0.603–0.810)	47.1	88.6	90.9%	40.8%
AAR	1.756	0.661 (0.554–0.768)	40.0	88.6	89.5%	37.8%

Table 3. Comparison of prediction model accuracies for severe PH. Abbreviations: MELD, Model of End-stage Liver Disease.

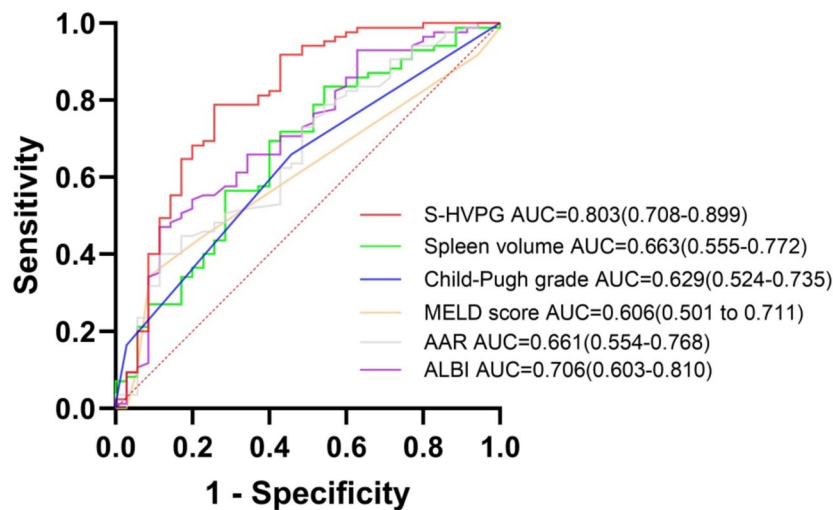


Fig. 4. Comparison of S-HVPG score with other methods in predicting severe PH.

analysis demonstrated significant associations ($P < 0.05$) between age, PLT, HB, INR, ALB, bleeding risk of esophageal varices, bleeding risk of gastric varices, spleen volume, and the occurrence of severe PH, suggesting these factors could independently contribute to the diagnosis of severe PH. The potential diagnostic indicators identified from the univariate logistic regression analysis underwent multivariate logistic regression analysis. This analysis revealed that age (OR = 1.054, 95% CI: 1.004–1.106, $p = 0.033$), albumin levels (OR = 0.877, 95% CI: 0.782–0.984, $p = 0.026$), and spleen volume (OR = 1.002, 95% CI: 1.001–1.004, $p = 0.041$) were independent diagnostic factors associated with severe PH (Table 2).

Derivation of the “S-HVPG” score

Based on multivariate logistic regression analysis, a clinical diagnostic model was developed for severe PH using HVPG ≥ 16 mmHg, termed the “S-HVPG” score. The formula for the model is $\text{logit}(P = \text{severe PH}) = 0.003 * \text{spleen volume} + 0.049 * \text{age} - 0.161 * \text{albumin} + 2.068$, where spleen volume is in cm^3 , age in years, and albumin in g/L.

Precision and Stability of the “S-HVPG” score

The Hosmer-Lemeshow test yielded a result of $p = 0.076$, and calibration curves demonstrated good agreement for the S-HVPG score, indicating no significant difference between predicted and observed values (S1 Fig). The S-HVPG score demonstrated superior diagnostic efficacy for identifying HVPG ≥ 16 mmHg, achieving an AUC of 0.803 (95% CI: 0.708–0.899), which significantly outperformed spleen volume alone, CP score, MELD score, ALBI, and AAR. At the optimal threshold of 0.694, the model exhibited balanced sensitivity (78.8%) and specificity (74.3%), with clinically meaningful predictive values: PPV = 88.2% and NPV = 59.1% (Table 3; Fig. 4). DCA curves showed that the S-HVPG score provided greater net clinical benefit compared to other models (S2 Fig). A cutoff value of 0.694 for the S-HVPG score yielded optimal sensitivity of 78.8% and specificity of 74.3% for distinguishing severe PH in cirrhotic patients.

Bootstrap internal validation confirmed higher and less variable AUC values for the model, AUC (95% CI) = 0.805 (0.796–0.814), indicating good precision and stability (S3 Fig).

Discussion

The natural course of cirrhosis is characterized by a silent, asymptomatic phase until elevated portal pressure and impaired hepatic function manifest into clinical phenotypes. The decompensated phase of cirrhosis is marked by prominent clinical signs, with ascites, bleeding, and hepatic encephalopathy being the most common. After initial signs of decompensation appear, the disease typically progresses more rapidly towards death or necessitates liver transplant^{1,23}. Measurement of HVPG via hepatic venous catheterization remains the gold standard for assessing portal hypertension in cirrhotic patients. HVPG values > 5 mmHg indicate sinusoidal portal hypertension; HVPG ≥ 10 mmHg defines “clinically significant portal hypertension”; HVPG ≥ 12 mmHg suggests a risk of variceal hemorrhage; HVPG ≥ 16 mmHg indicates a higher mortality risk; and HVPG ≥ 20 mmHg is associated with variceal bleeding, with ≥ 20 mmHg often leading to uncontrolled bleeding, early rebleeding, and mortality^{5,7,8}. However, due to drawbacks such as invasiveness and technical complexity, several studies have explored non-invasive methods to replace HVPG measurement, including serum biomarkers, angiomics, imaging techniques, liver stiffness measurement, and combinations thereof^{6,24–27}. Among these, significant advancements have been made in diagnosing CSPH using anatomical imaging. In patients with decompensated cirrhosis, monitoring HVPG reduces mortality and improves survival²⁸. One study showed that HVPG ≥ 16 mmHg was associated with persistent bleeding or rebleeding²⁹. In addition, Villanueva et al. noted that HVPG > 16 mmHg was a predictor of treatment failure³⁰. Xi-Xuan Wang’s study showed that patients with HVPG ≥ 16 mmHg had increased mortality from acute variceal bleeding, and that covered TIPS placement increased

long-term graft-free survival in patients admitted with HVPg ≥ 16 mmHg combined with variceal bleeding³¹. Nonetheless, research on non-invasive diagnosis of HVPg ≥ 16 mmHg remains limited^{32,33}. According to the Baveno VII consensus, patients at risk of endoscopic signs of portal hypertension can be predictively assessed using liver stiffness alone or in combination with PLT, spleen size, spleen stiffness, and other parameters⁵. This study aimed to investigate the correlation between spleen volume and HVPg in cirrhotic patients and develop a non-invasive model, combining clinical laboratory indices, to predict the risk of complications from difficult-to-control or recurrent decompensated cirrhosis and higher mortality rates.

Splenic size is recognized as a prognostic predictor in cirrhosis. Morphological changes in the spleen are common in cirrhotic patients, with approximately 60–65% exhibiting splenomegaly³⁴. Ascites, splenomegaly, and the development of collateral circulation are the three main clinical manifestations of portal hypertension³⁵. The clinical significance of portal hypertension arises from increased liver resistance to perfusion in advanced stages of chronic liver disease, particularly cirrhosis due to hepatic fibrosis. This leads to a compensatory rise in portal venous pressure transmitted retrogradely to the splenic veins, resulting in splenomegaly. Additionally, splenic vein blood flow obstruction in portal hypertension causes congestion and dilation of splenic sinuses, influencing spleen size^{34,36}. Previous studies have indicated that spleen volume can non-invasively diagnose CSPH in patients with hepatocellular carcinoma^{13,14}. Furthermore, one study demonstrated that spleen volume can diagnose HVPg > 12 mmHg in cirrhotic patients³⁷. However, to the best of our knowledge, no studies have specifically examined spleen volume as a diagnostic tool for portal hypertension in cirrhotic patients with HVPg ≥ 16 mmHg.

Our study revealed a moderate linear positive correlation between spleen volume and HVPg in cirrhotic patients, suggesting spleen volume can serve as a diagnostic indicator for assessing portal venous pressure magnitude in this population. This finding aligns closely with previous research¹⁴. However, the correlation coefficient obtained in our study was not as high as reported in other literature, likely due to the majority of cirrhotic patients included being in the decompensated stage with HVPg > 10 mmHg. Multivariate logistic regression analysis identified spleen volume, age, and albumin levels as independent predictors of severe PH. While both esophageal and gastric varices showed significant associations in univariate analysis, these associations were attenuated upon multivariate adjustment. The loss of significance for esophagogastric variceal bleeding risk in the multivariate analysis may be attributed to limited statistical power due to sample size constraints, which may reduce sensitivity to detect modest effects when adjusting for multiple predictors. The clinical relevance of these findings requires further validation in large-scale prospective studies. From this analysis, we constructed a clinical diagnostic model S-HVPg score: $\text{logit}(P = \text{severe PH}) = 0.003 * \text{spleen volume} + 0.049 * \text{age} - 0.161 * \text{albumin} + 2.068$. The S-HVPg score demonstrated a higher AUC value compared to spleen volume alone and outperformed other scores including the Child-Pugh score, MELD score, ABRI, and AAR, indicating superior diagnostic performance for non-invasive diagnosis of severe PH. Internal validation through Bootstrap resampling confirmed consistent diagnostic efficacy of the S-HVPg score. ROC curve analysis identified a cutoff value of 0.694 for diagnosing severe PH, achieving a sensitivity of 78.8% and specificity of 74.3%. The model achieved a PPV of 88.2%. This high PPV indicates precise identification of severe portal hypertension, supporting its utility as a clinical decision-aid tool. In resource-constrained settings with limited access to hemodynamic monitoring, this performance translates to reduced requirements for invasive HVPg measurements. The Hosmer-Lemeshow test showed $p > 0.05$, suggesting acceptable calibration of the model. DCA further demonstrated that the S-HVPg score provided greater net clinical benefit compared to alternative models. The model was additionally validated for HVPg thresholds of ≥ 10 mmHg and ≥ 12 mmHg, demonstrating AUCs of 0.890 and 0.835, respectively; however, the limited sample sizes in these subgroups precluded further analysis in this study (unpublished data).

The innovations of this study are twofold. Firstly, we proposed the diagnosis of severe PH in cirrhotic patients with HVPg ≥ 16 mmHg for the first time. Secondly, we constructed a non-invasive model using spleen volume to diagnose severe PH, demonstrating a high AUC value and moderate diagnostic accuracy. However, there are several limitations in this research. Firstly, it was a single-center cross-sectional study with a limited number of cases, potentially introducing bias into the results. Secondly, the study population had a complex etiology, with relatively small numbers of cases for each etiology. Thirdly, external validation and prospective studies were lacking. Therefore, further research is essential to validate our findings.

In summary, we developed a non-invasive diagnostic model for severe PH based on spleen volume. This model exhibits good diagnostic accuracy and offers a straightforward, reliable, safe, and non-invasive initial screening tool for clinicians to assess severe PH in cirrhotic patients.

Data availability

The datasets generated during and/or analysed during the current study are available from the corresponding author on reasonable request.

Received: 29 December 2024; Accepted: 12 May 2025

Published online: 15 May 2025

References

- Ginès, P. et al. Liver cirrhosis. *Lancet* **398**, 1359–1376. [https://doi.org/10.1016/s0140-6736\(21\)01374-x](https://doi.org/10.1016/s0140-6736(21)01374-x) (2021).
- Engelmann, C., Clària, J., Szabo, G., Bosch, J. & Bernardi, M. Pathophysiology of decompensated cirrhosis: portal hypertension, circulatory dysfunction, inflammation, metabolism and mitochondrial dysfunction. *J. Hepatol.* **75** (Suppl 1), S49–s66. <https://doi.org/10.1016/j.jhep.2021.01.002> (2021).
- Heo, S. et al. CT Rule-in and Rule-out criteria for clinically significant portal hypertension in chronic liver disease. *Radiology* **309**, e231208. <https://doi.org/10.1148/radiol.231208> (2023).

4. Kaplan, D. E. et al. AASLD practice guidance on risk stratification and management of portal hypertension and varices in cirrhosis. *Hepatology* **79**, 1180–1211. <https://doi.org/10.1097/hep.0000000000000647> (2024).
5. de Franchis, R., Bosch, J., Garcia-Tsao, G., Reiberger, T. & Ripoll, C. Baveno VII - Renewing consensus in portal hypertension. *J. Hepatol.* **76**, 959–974. <https://doi.org/10.1016/j.jhep.2021.12.022> (2022).
6. Jindal, A. et al. Assessment of the performance of Non-invasive criteria for the evaluation of clinically significant portal hypertension in patients with compensated advanced chronic liver disease. *Dig. Dis. Sci.* **68**, 2149–2157. <https://doi.org/10.1007/s10620-022-07778-0> (2023).
7. Wang, H. L. & Sun, J. H. [Role of hepatic venous pressure gradient in the overall management process of portal hypertension]. *Zhonghua Gan Zang Bing Za Zhi*. **28**, 728–731. <https://doi.org/10.3760/cma.j.cn501113-20200613-00313> (2020).
8. Suk, K. T. Hepatic venous pressure gradient: clinical use in chronic liver disease. *Clin. Mol. Hepatol.* **20**, 6–14. <https://doi.org/10.3350/cmh.2014.20.1.6> (2014).
9. Tseng, Y. et al. Non-invasive predictive model for hepatic venous pressure gradient based on a 3-dimensional computed tomography volume rendering technology. *Exp. Ther. Med.* **15**, 3329–3335. <https://doi.org/10.3892/etm.2018.5816> (2018).
10. Liu, S. et al. Novel serum biomarker of golgi protein 73 for the diagnosis of clinically significant portal hypertension in patients with compensated cirrhosis. *J. Med. Virol.* **96**, e29380. <https://doi.org/10.1002/jmv.29380> (2024).
11. Garcia-Tsao, G., Abraldes, J. G., Berzigotti, A. & Bosch, J. Portal hypertensive bleeding in cirrhosis: risk stratification, diagnosis, and management: 2016 practice guidance by the American association for the study of liver diseases. *Hepatology* **65**, 310–335. <https://doi.org/10.1002/hep.28906> (2017).
12. Qi, X., Berzigotti, A., Cardenas, A. & Sarin, S. K. Emerging non-invasive approaches for diagnosis and monitoring of portal hypertension. *Lancet Gastroenterol. Hepatol.* **3**, 708–719. [https://doi.org/10.1016/s2468-1253\(18\)30232-2](https://doi.org/10.1016/s2468-1253(18)30232-2) (2018).
13. Romero-Cristóbal, M. et al. CT-derived liver and spleen volume accurately diagnose clinically significant portal hypertension in patients with hepatocellular carcinoma. *JHEP Rep.* **5**, 100645. <https://doi.org/10.1016/j.jhepr.2022.100645> (2023).
14. Iranmanesh, P. et al. Accurate computed tomography-based portal pressure assessment in patients with hepatocellular carcinoma. *J. Hepatol.* **60**, 969–974. <https://doi.org/10.1016/j.jhep.2013.12.015> (2014).
15. Sun, X. et al. Bibliometric-analysis visualization and review of non-invasive methods for monitoring and managing the portal hypertension. *Front. Med. (Lausanne)*. **9**, 960316. <https://doi.org/10.3389/fmed.2022.960316> (2022).
16. [Chinese guidelines on the management of liver cirrhosis]. *Zhonghua Gan Zang Bing Za Zhi* **27**, 846–865, doi:<https://doi.org/10.3760/cma.j.issn.1007-3418.2019.11.008> (2019).
17. Reiniš, J. et al. Assessment of portal hypertension severity using machine learning models in patients with compensated cirrhosis. *J. Hepatol.* **78**, 390–400. <https://doi.org/10.1016/j.jhep.2022.09.012> (2023).
18. [Consensus on clinical application of hepatic venous pressure gradient in China. *Zhonghua Yi Xue Za Zhi* **103**, 3885–3895, (2023). edition)] <https://doi.org/10.3760/cma.j.cn112137-20230831-00342> (2023).
19. Tajiri, T. et al. General rules for recording endoscopic findings of esophagogastric varices (2nd edition). *Dig Endosc* **22**, 1–9, (2010). <https://doi.org/10.1111/j.1443-1661.2009.00929.x>
20. Beppu, K. et al. Prediction of variceal hemorrhage by esophageal endoscopy. *Gastrointest. Endosc.* **27**, 213–218. [https://doi.org/10.1016/s0016-5107\(81\)73224-3](https://doi.org/10.1016/s0016-5107(81)73224-3) (1981).
21. Welsh, P. et al. Derivation and validation of a 10-Year risk score for symptomatic abdominal aortic aneurysm: cohort study of nearly 500 000 individuals. *Circulation* **144**, 604–614. <https://doi.org/10.1161/circulationaha.120.053022> (2021).
22. Guo, Y., Shen, B., Xue, Y. & Li, Y. Development and validation of a non-invasive model for predicting significant fibrosis based on patients with nonalcoholic fatty liver disease in the united States. *Front. Endocrinol. (Lausanne)*. **14**, 1207365. <https://doi.org/10.3389/fendo.2023.1207365> (2023).
23. EASL Clinical Practice Guidelines for the management of patients. With decompensated cirrhosis. *J. Hepatol.* **69**, 406–460. <https://doi.org/10.1016/j.jhep.2018.03.024> (2018).
24. Procopet, B. et al. Serum tests, liver stiffness and artificial neural networks for diagnosing cirrhosis and portal hypertension. *Dig. Liver Dis.* **47**, 411–416. <https://doi.org/10.1016/j.dld.2015.02.001> (2015).
25. Procopet, B. et al. Real-time shear-wave elastography: applicability, reliability and accuracy for clinically significant portal hypertension. *J. Hepatol.* **62**, 1068–1075. <https://doi.org/10.1016/j.jhep.2014.12.007> (2015).
26. Berzigotti, A. et al. Reliability of the Estimation of total hepatic blood flow by doppler ultrasound in patients with cirrhotic portal hypertension. *J. Hepatol.* **59**, 717–722. <https://doi.org/10.1016/j.jhep.2013.04.037> (2013).
27. Wang, C. et al. Diagnosis of clinically significant portal hypertension using CT- and MRI-based vascular model. *Radiology* **307**, e221648. <https://doi.org/10.1148/radiol.221648> (2023).
28. Zeng, X. et al. Skeletal muscle alterations indicate poor prognosis in cirrhotic patients: a multicenter cohort study in China. *Hepatol. Int.* **18**, 673–687. <https://doi.org/10.1007/s12072-023-10497-x> (2024).
29. Ready, J. B., Robertson, A. D., Goff, J. S. & Rector, W. G. Jr. Assessment of the risk of bleeding from esophageal varices by continuous monitoring of portal pressure. *Gastroenterology* **100**, 1403–1410 (1991).
30. Villanueva, C. et al. A randomized controlled trial comparing ligation and sclerotherapy as emergency endoscopic treatment added to somatostatin in acute variceal bleeding. *J. Hepatol.* **45**, 560–567. <https://doi.org/10.1016/j.jhep.2006.05.016> (2006).
31. Wang, X. X. et al. Pre-transjugular-intrahepatic-portosystemic-shunt measurement of hepatic venous pressure gradient and its clinical application: A comparison study. *World J. Gastroenterol.* **29**, 3519–3533. <https://doi.org/10.3748/wjg.v29.i22.3519> (2023).
32. Liu, F. et al. Development and validation of a radiomics signature for clinically significant portal hypertension in cirrhosis (CHESS1701): a prospective multicenter study. *EBioMedicine* **36**, 151–158. <https://doi.org/10.1016/j.ebiom.2018.09.023> (2018).
33. Yu, Q. et al. An imaging-based artificial intelligence model for non-invasive grading of hepatic venous pressure gradient in cirrhotic portal hypertension. *Cell. Rep. Med.* **3**, 100563. <https://doi.org/10.1016/j.xcrm.2022.100563> (2022).
34. Wang, P., Hu, X. & Xie, F. Predictive value of liver and spleen stiffness measurement based on two-dimensional shear wave elastography for the portal vein pressure in patients with compensatory viral cirrhosis. *PeerJ* **11**, e15956. <https://doi.org/10.7717/peerj.15956> (2023).
35. Etzion, O. et al. Spleen and liver volumetrics as surrogate markers of hepatic venous pressure gradient in patients with noncirrhotic portal hypertension. *Hepatol. Commun.* **2**, 919–928. <https://doi.org/10.1002/hep4.1198> (2018).
36. Helgeson, S. et al. Spleen volume is independently associated with non-alcoholic fatty liver disease, liver volume and liver fibrosis. *Heliyon* **10**, e28123. <https://doi.org/10.1016/j.heliyon.2024.e28123> (2024).
37. Yan, S. P. et al. A new model combining the liver/spleen volume ratio and classification of varices predicts HVP in hepatitis B patients with cirrhosis. *Eur. J. Gastroenterol. Hepatol.* **27**, 335–343. <https://doi.org/10.1097/meg.0000000000000269> (2015).

Acknowledgements

This research was supported by the Tianjin Key Medical Discipline (Specialty) Construction Project (Grant No. TJYXZDXK-034A) and the Tianjin Health Research Project. (Grant No. TJWJ2022XK029).

Author contributions

Study design: Xinyu Chen, Huiling Xiang, Yicheng lin, Qing Ye. Performance of experiments: Xinyu Chen, Jiamei Zhou, Yicheng lin, Fenghui Li. Analysis and interpretation of data: Xinyu Chen, Jiamei Zhou, Kefeng

Jia, Jiajun Tian, Rong Lv, Weili Yin, Fang Wang, Ping Zhu. Manuscript writing: Xinyu Chen, Chao Yang, Jiayin Wang, Tao Wang. Critical revision: Huiling Xiang, Ying Liu, Qing Ye. Statistical analysis: Xinyu Chen, Junqing Yan, Ying Liu. Critical funding: Huiling Xiang.

Declarations

Competing interests

The authors declare no competing interests.

Conflict of interest

The authors have no conflict of interests related to this publication.

Ethics approval

This study protocol conforms to the ethical guidelines of the 1975 Declaration of Helsinki. This study was approved by the Ethics Committee of Tianjin Third Central Hospital on April 22, 2019 (IRB2019-022-04).

Informed consent

This retrospective analysis utilized fully anonymized clinical data, with all personally identifiable information irreversibly removed prior to analysis. Informed consent was waived by the Ethics Committee of Tianjin Third Central Hospital/IRB2019-022-04.

Additional information

Supplementary Information The online version contains supplementary material available at <https://doi.org/10.1038/s41598-025-02143-3>.

Correspondence and requests for materials should be addressed to Q.Y. or H.X.

Reprints and permissions information is available at www.nature.com/reprints.

Publisher's note Springer Nature remains neutral with regard to jurisdictional claims in published maps and institutional affiliations.

Open Access This article is licensed under a Creative Commons Attribution-NonCommercial-NoDerivatives 4.0 International License, which permits any non-commercial use, sharing, distribution and reproduction in any medium or format, as long as you give appropriate credit to the original author(s) and the source, provide a link to the Creative Commons licence, and indicate if you modified the licensed material. You do not have permission under this licence to share adapted material derived from this article or parts of it. The images or other third party material in this article are included in the article's Creative Commons licence, unless indicated otherwise in a credit line to the material. If material is not included in the article's Creative Commons licence and your intended use is not permitted by statutory regulation or exceeds the permitted use, you will need to obtain permission directly from the copyright holder. To view a copy of this licence, visit <http://creativecommons.org/licenses/by-nc-nd/4.0/>.

© The Author(s) 2025